

© 2020 Wiley-VCH GmbH

ADVANCED HEALTHCARE MATERIALS

Supporting Information

for *Adv. Healthcare Mater.*, DOI: 10.1002/adhm.202000782

Optimizing Bifurcated Channels within an Anisotropic Scaffold for Engineering Vascularized Oriented Tissues

Yongcong Fang, Liliang Ouyang, Ting Zhang, Chengjin Wang, Bingchuan Lu, and Wei Sun*

Supporting Information

Optimizing Bifurcated Channels within an Anisotropic Scaffold for Engineering Vascularized Oriented Tissues

Yongcong Fang, Liliang Ouyang, Ting Zhang, Chengjin Wang, Bingchuan Lu, Wei Sun*

Table of Contents

Supplementary Methods

Oxygen Diffusion Coefficient Measurement

Hydraulic Permeability Measurement

Mechanical Analysis

Immunostaining

DNA Quantification

Supplementary Figures

Figure S1. The schematic diagram of the fabrication of the cellular construct.

Figure S2. Sacrificial template fabrication and channel characterization.

Figure S3. Morphology of porous polymer membrane.

Figure S4. The characterization of lumen endothelialization.

Figure S5. Characterization of C2C12s-seeded oriented scaffolds by staining.

Figure S6. Simulation of shear stress distribution within bifurcated channels.

Supplementary Tables

Table 1. Parameters used to simulate oxygen concentration profiles.

Supplementary Methods

Oxygen Diffusion Coefficient Measurement

An experimental apparatus modified from a conventional diffusion measurement system was constructed to determine the effective oxygen diffusion coefficient ($D_{e,s}$). Briefly, the apparatus consisted of two chambers filled with culture medium and separated by the porous scaffold. The donor chamber was supplied with fresh saturated culture medium via a peristaltic tubing system to maintain a saturated oxygen concentration. This setup allowed oxygen molecules to diffuse from the donor chamber to the receiver chamber through the porous scaffold. The apparatus was placed on a stirring hot plate to maintain the temperature at 37 °C during measurement. The change in oxygen concentration in the receiver chamber was measured using an oxygen probe (RDO™ Optical Dissolved Oxygen Sensor, Thermo Scientific, USA) every 5 min for 100 min with an initial oxygen concentration below 2 mg L⁻¹. Although the variation was less than 0.5 mg L⁻¹, the saturated oxygen concentration in the donor chamber was also measured for each experiment. The measured oxygen concentration data were used to calculate the effective oxygen diffusion coefficient ($D_{e,s}$).

Hydraulic Permeability Measurement

An experimental setup based on Darcy's Law was prepared to determine hydraulic permeability. Briefly, the scaffold was fitted into a chamber connected to the water reservoir via a silicon tube using a rubber gasket. Water flow from the water reservoir to the chamber was provided by gravity. The fixed vertical distance from the chamber to the surface of the water in the reservoir resulted in a constant pressure. The flow rate was

calculated by measuring the volume of the water that accumulated in the beaker over 30 s and hydraulic permeability was calculated from at least three scaffolds.

Mechanical Analysis

Scaffold mechanical properties were evaluated using the uniaxial stretch with a mechanical testing machine (ELF3200, Bose, USA). Scaffold samples were cut into rectangular pieces (10 mm × 15 mm × 2 mm), hydrated in PBS solution until testing, then secured at opposite ends onto customized clamps. Samples were preconditioned for ten cycles at a 0.05 mm min⁻¹ rate with a 0.05 N preload. This was followed by 0.1 mm min⁻¹ uniaxial stretching. The load and displacement data were collected at a frequency of 2 Hz. The stress-strain plot was processed and the elastic modulus was calculated using 5%–20% strain.

Immunostaining

Immunostaining was performed to evaluate the morphological features of cellular constructs. Briefly, the cellular constructs were rinsed with PBS, fixed with 4% paraformaldehyde solution, rinsed with PBS again, then permeabilized with 0.1% Triton X-100 followed by blocking with 10% bovine serum albumin (Calbiochem, USA). To visualize endothelial cells, the HUVEC-laden samples were incubated with anti-CD31 (1:100 dilution, Rabbit mAb, Abcam) primary antibody at 4°C overnight, followed by PBS washing and further incubation with goat anti-rabbit secondary antibody (1:500 dilution, Alexa Fluor 594, Invitrogen) diluted in 1% BSA for 2 h at room temperature. Samples were then counterstained with 4',6-diamidino-2-phenylindole (DAPI, GBI Labs, 0.5 mg mL⁻¹) for 15 min before imaging. Cellular samples were optionally stained with Phalloidin-iFluor 488 (0.5 mg mL⁻¹, Abcam) for 1 h at room temperature to visualize

cytoskeleton. Confocal microscopy was performed using an inverted Zeiss LSM 880 (Zeiss, Germany) microscope with 4× and 10× magnification objectives.

DNA Quantification

The cellular constructs were harvested on day 3. Total DNA was extracted by digesting the cellular constructs in a proteinase K solution (Yeasen, China) at 56 °C for 16 h, followed by three freeze-thaw cycles (10 min at -70 °C and 10 min at 36 °C, respectively). After centrifugation at 13,000 rpm and 4 °C for 15 min, the supernatant was removed and the DNA pellets were resuspended in distilled water. Finally, the DNA content was measured at 260 nm using a spectrophotometer (ND1000, NanoDrop Technologies, USA).

Supplementary Figures

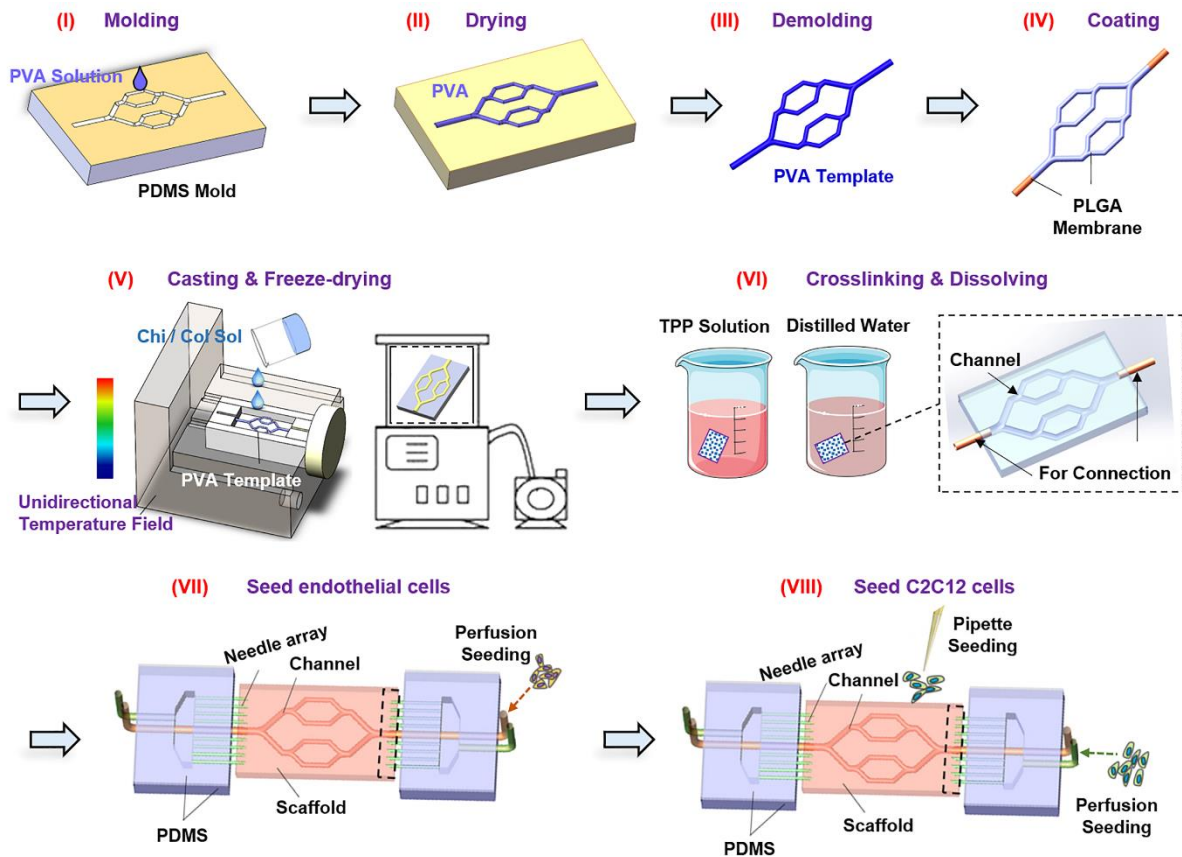


Figure S1. The schematic diagram of the fabrication of the cellular construct.

I) Aqueous PVA solution casted on the PDMS mold and allowed to dry overnight; II-III) The dried PVA layer (II) gently demolded to generate the PVA template (III); IV) The PVA template further coated with polymer membrane by immersion in a 25 mg mL^{-1} solution of poly(D, L-lactide-co-glycolide) (PLGA) in chloroform; V) Chitosan/Collagen solution casted in custom-made mold with PVA template embedded and frozen at $-20 \text{ }^\circ\text{C}$ under unidirectional temperature field; The frozen scaffold freeze-dried for 48 h to generate oriented macro-pores; VI) The scaffold crosslinked with sodium-polyphosphate (TPP) solution, and dissolved in distilled water to generate channel network; VII) Endothelial cells seeded into the channel networks by perfusion seeding method; IX)

After incubation, C2C12s seeded into the porous zone by a combination of needle array-assisted perfusion seeding and pipette seeding on the surface to obtain a uniform cell distribution. The bioreactor was perfused with mixed culture medium through the channel network to provide nutrient and oxygen to the cellular construct.

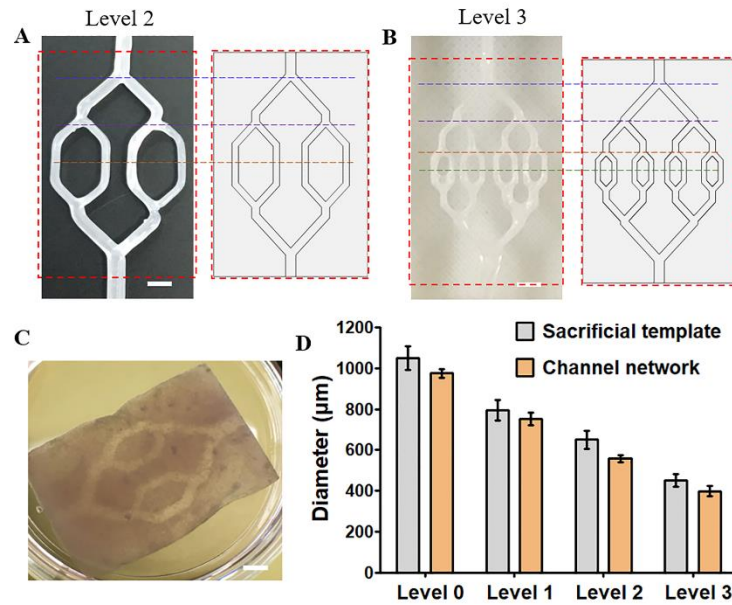


Figure S2. Sacrificial template fabrication and channel characterization.

The fabricated PVA templates with bifurcation levels A) 2 and B) 3. C) The chitosan/collagen scaffold after crosslinking and sacrificial template dissolution (scale bar: 1 mm). D) Changes in diameter between the sacrificial templates and bifurcated channels.

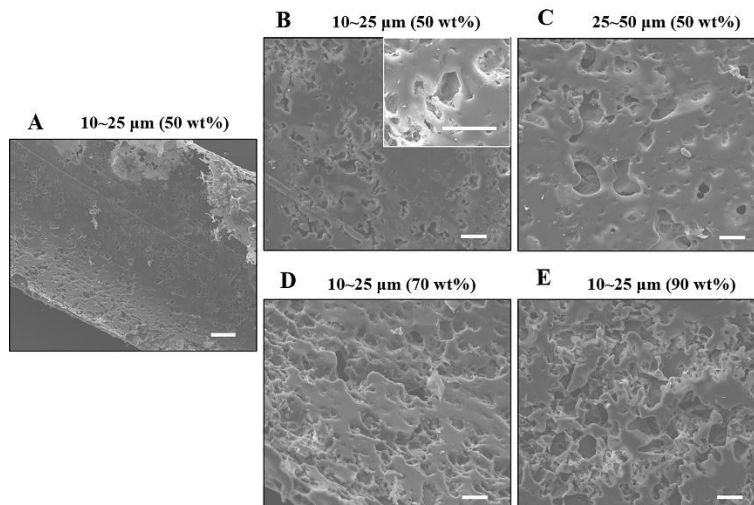


Figure S3. Morphology of porous polymer membrane.

The sizes and weight ratios of NaCl porogen particles: A, B) 10–25 μm , 50 wt%, C) 25–50 μm , 50 wt%, D) 10–25 μm , 70 wt%, and E) 10–25 μm , 90 wt%, respectively. Scale bars: A) 100 μm , B-E) 25 μm .

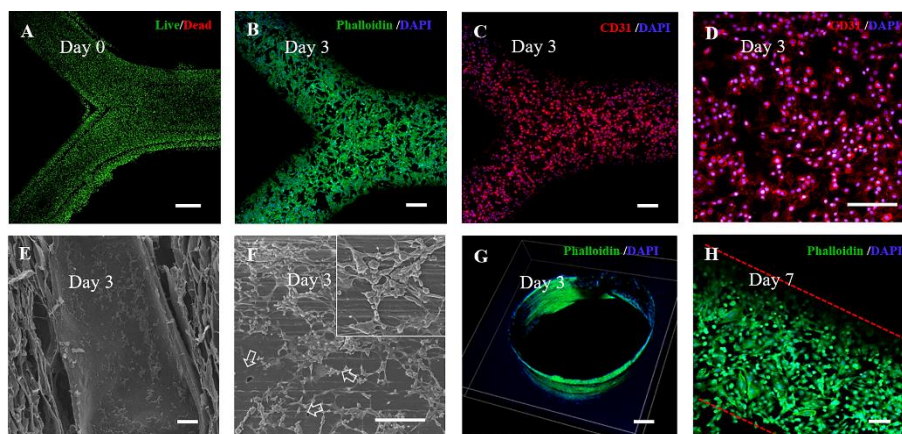


Figure S4. The characterization of lumen endothelialization.

A) Live/dead staining on day 0 showing HUVECs distribution. B) F-actin immunostaining on day 3 showing HUVECs morphology. C,D) CD31 immunostaining on day 3 revealing the specific tight junction of HUVECs. E,F) SEM images showing channel surface morphology on day 3 with inset of HUVECs distribution. The white

arrows pointing to the micro-holes on the channel surface. G) Reconstructed tubular structure from F-actin immunostaining on day 3. H) F-actin immunostaining on day 7 showing a confluent monolayer lining the channel surface. Scale bars: A-H) 100 μm .

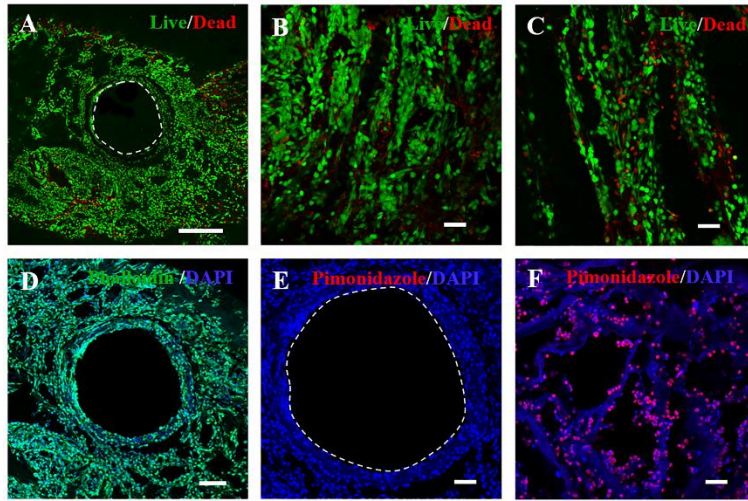


Figure S5. Characterization of C2C12s-seeded oriented scaffolds by staining.

Live/dead staining on day 1 showing cell viability at A) cross-section and B-C) longitudinal sections. B) and C) indicate positions near and away from the channels, respectively. D) F-actin immunostaining on day 3 at a cross-section showing the cell morphology near the channels. Cross-section images of pimonidazole staining on day 3 showing hypoxic cells E) near and F) away from the channels. Scale bars: A) 500 μm , B-C, E-F) 100 μm , D) 200 μm .

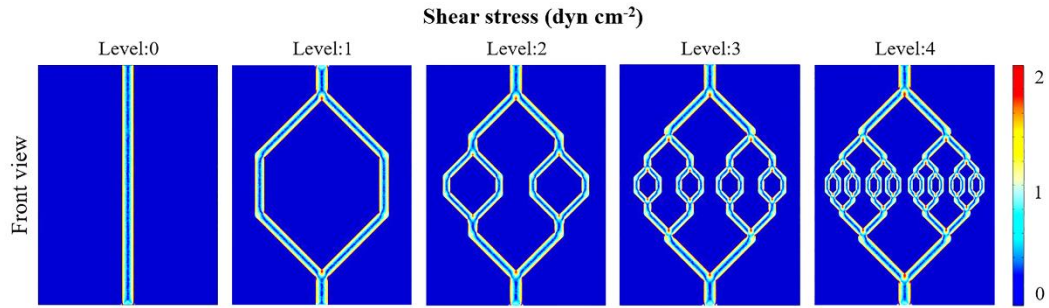


Figure S6. Simulation of shear stress distribution within bifurcated channels.

Supplementary Tables

Table 1. Parameters used to simulate oxygen concentration profiles.

Parameters	Values	Sources
Hydraulic Permeability_Parallel: K_P	$5.05 \times 10^{-12} \text{ m}^2$	measured
Hydraulic Permeability_Vertical: K_V	$1.11 \times 10^{-12} \text{ m}^2$	measured
Effective Diffusion Coefficient_Parallel: D_P	$1.52 \times 10^{-5} \text{ cm}^2 \text{ s}^{-1}$	measured
Effective Diffusion Coefficient_Vertical: D_V	$2.32 \times 10^{-6} \text{ cm}^2 \text{ s}^{-1}$	measured
Porosity	0.72	measured
Oxygen Diffusion Coefficient in Culture Medium: D_M	$3.83 \times 10^{-5} \text{ cm}^2 \text{ s}^{-1}$	ref 28,b
Maximum Oxygen Uptake Rate: $V_{O_2\text{max}}$	$2.5 \times 10^{-17} \text{ mol cell}^{-1} \text{ s}^{-1}$	ref 28,b
Michaelis–Menten Constant: K_m	$6.875 \text{ } \mu\text{mol L}^{-1}$	ref 28,b
Oxygen Concentration at the Boundary: C_{oxy}	$222.5 \text{ } \mu\text{M}$	ref 28,b
Inlet Oxygen Concentration: C_{inlet}	$222.5 \text{ } \mu\text{M}$	ref 28,b
Viscosity of Culture Medium: μ	$8.4 \times 10^{-4} \text{ kg m}^{-1} \text{ s}^{-1}$	ref 28,b
Cell Seeding Density: N_{cell}	$5 \times 10^6 \text{ cell cm}^{-3}$	set
Diameter at the inlet: D_{inlet}	$1.0 \times 10^{-3} \text{ m}$	set
Flow Velocity at the inlet: V_{inlet}	$2.12 \times 10^{-4} \text{ m s}^{-1}$	set